A New Angle on Energy Optimization of a microFIT PV System

by

Patrick James McVey White

Submitted to

Karin Hinzer

ELG 6373

Contents

List of Figures

I. Introduction

Ottawa is home to the larges amount of solar energy capacity per province, as seen in Fig. 1. In 2009, the government of Ontario introduced the microFIT program to encourage small-scale residential deployment of renewable energies project. It promises a 20-year set price for electricity generation. Optimizing the flat panel PV system can increase the total energy by 6.19% with a variable collector tilt instalment. This equates to an absolute gain of $709.70 in annual revenue. This report will thoroughly analyse the parameters of a flat panel PV energy yield calculation with a goal to generate the highest return of investment through maximizing the total amount of sunshine on the panel.

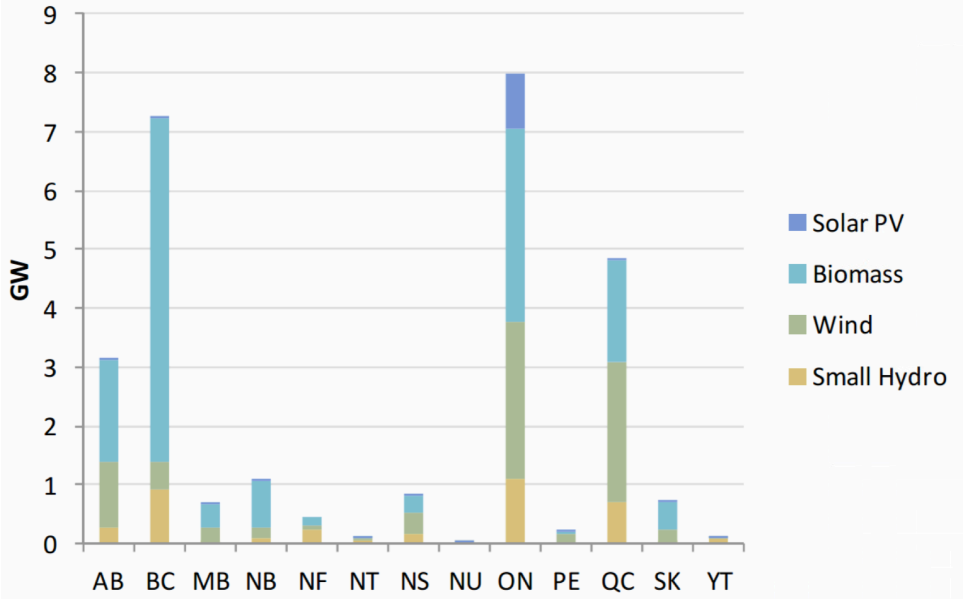

Fig. 1. Renewable Energy Capacity by Province [1]

II. The Solar Resource

The sun is an abundant source of energy. The average light intensity it produces is 1353 W/m^2 outside the atmosphere and 0.2 kW/m^2 24-hour annual averages over the surface of the earth [1]. Understanding this resource is a crucial component to analysing a photovoltaic system. This section will first describe the sun as a simple source outside the atmosphere and then the components that effect the propagation of light that results in the terrestrial components of the sun.

II.I. Blackbody Radiation

All objects with a temperature above absolute zero emit radiation. The sun's radiation at its surface is approximately that of a blackbody at 5780 K [1]. A blackbody is both an ideal emitter and absorber of radiation and its energy can be described by Plank's distribution. The spectral irradiance quantifies the power density on a surface per wavelength, $W/m^2/nm$. The sun is a broadband source emitting radiation over a large wavelength range. 97% of the total intensity is within the ultraviolet, visible, and infrared or 290 nm to 3000 nm on the radiation spectrum [3]. In reference to Fig. 2, the spectral irradiance of a blackbody shifts to shorter wavelengths as temperature increases.

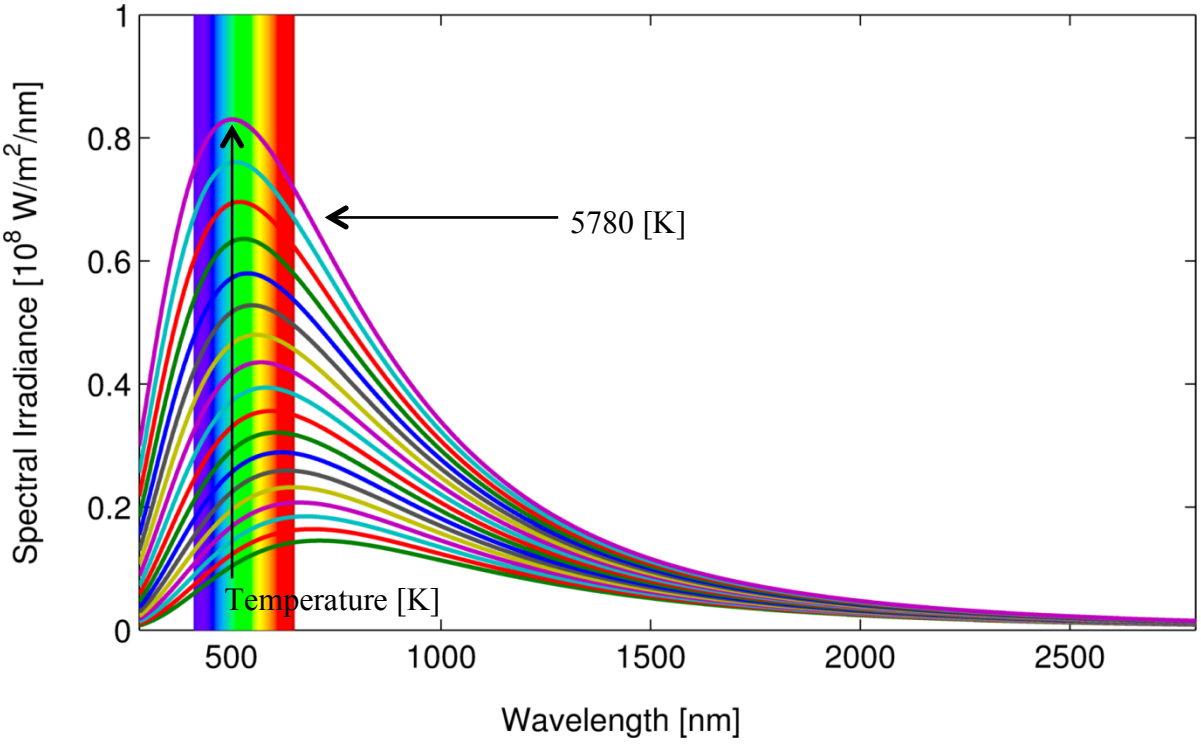

Fig. 2. The spectral irradiance of a blackbody emitter as temperature is increased from 4080 K to 5780 K

II.II. Extra-Terrestrial Radiation

The Total Solar Irradiance (TSI) at the sun's surface is relatively constants and dependent on the number of suns spots; the solar activity follows an eleven year cycle [3]. The total power density that reaches the earth's atmosphere is dependent on its separation. The Extra-Terrestrial Radiation (ETR) is calculated using equation (1),

$$I_{ETR} = TSI * r_e \ \left[W / m^2\right] \ (1)$$

where,

$$r_e = 1.0011 + 0.034221\cos\xi + 1.28\text{x}10^{-3}\sin\xi + 7.19\text{x}10^{-4}\cos 2\xi + 7.7\text{x}10^{-5}\sin 2\xi$$

$$\xi = \frac{2\pi d}{365} radians$$

The earth's orbit draws out an elliptical pattern on a horizontal plane through the middle of the sun. Therefore, the distance between the sun and the earth varies as a function of time. The two extremes are in January and July when the earth is closest and furthest from the sun, respectively. Measured satellite data over the past 24 years, the average TSI for, solar application, at the earth's atmosphere is 1366.1 W/m^2 [4]. In reference to Fig. 3, the daily variation of ETR for 2015 can be seen with a total annual fluctuation of 6.8%. On January 2nd, the ETR is 1414.0 W/m^2 and 1320.5 W/m^2 on July 3rd, a fluctuation of +3.5% and -3.3%, respectively.

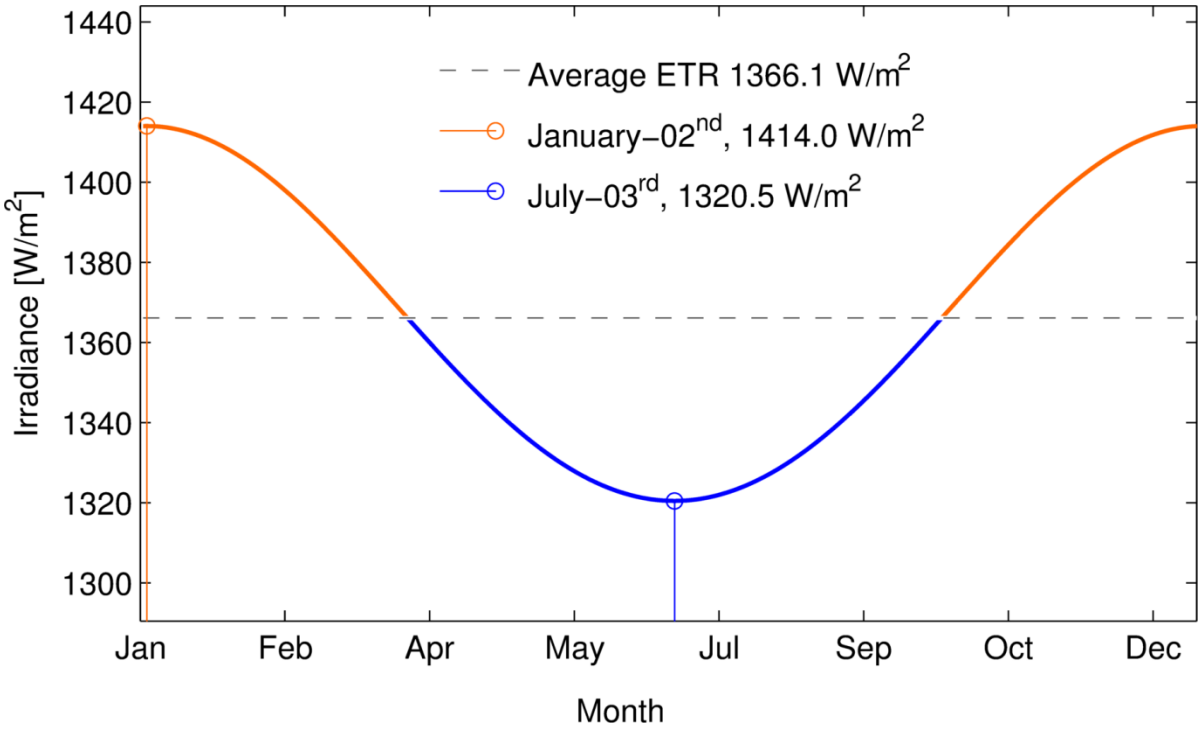

Fig. 3. The Extra-Terrestrial Radiation for 2015 where orange represents the sections of the year where the Extra-Terrestrial Radiation is greater than the average, 1366.1 W/m^2 or dashed line, and the blue region represent when the Extra-Terrestrial Radiation is less than the average. The maximum and minimum are on January 2nd and July 3rd with a difference of +3.5% and -3.3% of the average.

II.III. Solar Coordinates

To a stationary observer, the sun traverses east to west at a speed of 15^0/hr from sunrise to sunset. The celestial sphere is an imaginary sphere around the earth and used to describe the locations of the stars, sun, and planets in space from the perspective of the earth [5]. The horizontal plane through the earth's equator is the celestial equator and axis of the earth rotation is the polar axes. On the celestial sphere, the right ascending and declination angles characterize the sun. The right ascending angle is a measure of the sun's location on the horizontal plane through the celestial sphere. The declination angle measures the location above or below the horizontal plane through the celestial sphere plane. The tilt of the earth's axes is 23.44^0, the result is a fluctuation of the declination angle of $\pm 23.44^0$ over the year. The equinox, occurring twice a year, is the intersection of the earth's orbit plane and the celestial equator [5]. At the equinox, the declination angle is therefore 0. During the summer, the sun is above the equatorial resulting in positive an angle that reaches the maximum of 23.44^0 on the summer solstice. During the winter, the sun is below the equatorial that reaches the minimum of -23.44^0 on the winter solstice. This fluctuation can be seen in Fig. 2. The declination angle for any given day number, n, can be calculated for any day as,

$$\delta = 0.006918 - 0.399912\cos\xi + 0.070257\sin\xi - 0.00678\cos 2\xi + 0.000907\sin 2\xi \quad (2)$$

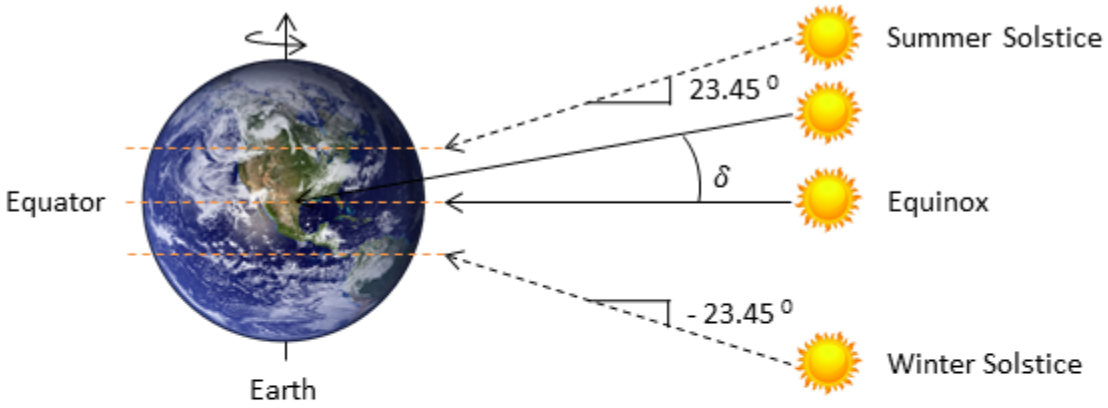

Fig. 4. The declination of the sun at the Equinox, Summer and Winter solstice, and for an arbitrary day during the summer. The declination varies over the year from $\pm 23.44^0$.

At specific latitude on the earth, the meridional plane defines the relationship to the celestial sphere. The meridional plane is perpendicular to the local east-west axis and passes through the earth`s axis of rotation and is defined by due south, due north and the zenith [5]. Now, a coordinate system that describes the sun`s location with respect to a fixed observer on the meridional plane can be viewed in Fig. 5. The azimuth, φ_s, is measured from north towards the east. The elevation angle, β, describes the angle from the horizontal to the sun`s position for a specified azimuth. The sun`s zenith angle is measured from the normal of the local meridional plane. These angles can be calculated independently as,

$$\sin(\beta) = \sin(\mathrm{LAT})\sin(\delta) + \cos(\mathrm{LAT})\cos(\delta)\cos(H) \quad (3)$$

where,

$$H = 15^0(st - 12)$$

and

$$\sin(az) = \frac{-\cos(\delta)\sin(H)}{\cos(\pi/2 - \beta + 90)} \quad (4)$$

where H is the hour angle and LAT is the latitude of the local meridional plane. The hour angle is a measure of the amount of degrees between the equatorial plane and the sun. Solar time, *st,* is based on the sun position in the sky. Solar time can be calculated from the local time as,

$$st = lst + EoT + \frac{long_{sm} - long_{ob}}{15} \quad (5)$$

where *lst* is the local solar time, EoT, is the equation of time, L_{sm}.and L_{ob} is the longitude of the standard meridian and location of the observer, respectively. The bisection of these two are known a solar noon [5]. By convention, the azimuth angle is positive for angle before due south and negative after.

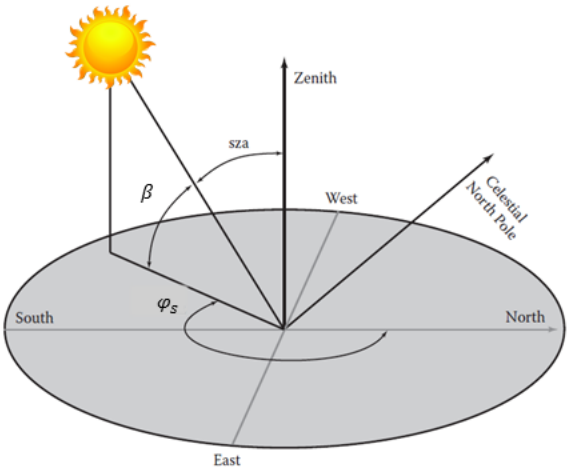

Fig. 5. The sun`s position for a fixed point on a meridian plane. The azimuth angle is measured from the north to the solar position on horizon. The elevation angle is a measure from the horizontal to the sun position.

II.IV. Air Mass

Dirt, gases, and aerosols affect the sun's intensity as light propagates to the surface of the earth. The light is filtered by the ozone, oxygen, water vapours, and carbon dioxide found in the atmosphere. The Air Mass (AM) is the path length the light must passes through normalized to the shorted possible path length relative to the observer. The AM can be calculated with equation (6) with the sun's elevation angle. Conventionally, an AM of 1 is defined at sea level. AM0, AM1, AM1.5 and AM2.0 can be seen in Fig. 6.

$$AM = \frac{1}{\cos(90-\beta)} \quad (6)$$

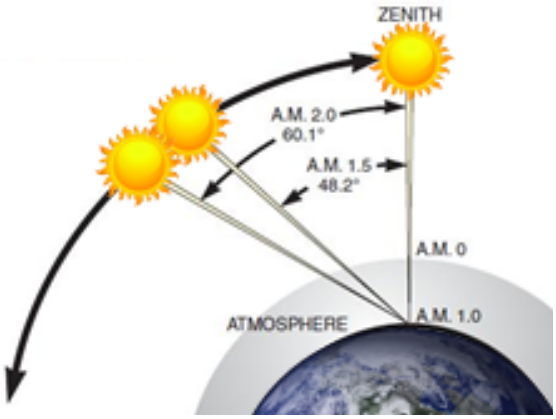

Fig. 6. The path length of light at sea level for an elevation angle of 90^0, 29.9^0, and 41.8^0

II.V. Terrestrial Radiation

The extra-terrestrial radiation is propagates freely in space until it reaches the earth's atmosphere. The molecules, arousals, and clouds in the atmosphere strongly influence the solar radiation that reaches the earth's surface. Without the presence of clouds, at solar noon 75 % of the extra-terrestrial radiation will reach the earth's surface with little attenuate [5]. This is the total radiation that passes directly through the atmosphere with no scattering or absorption is the *direct normal irradiance (DNI)*. Scattering will reflect some of the light back into space, the portion that reaches the earth's surface is the *diffuse horizontal irradiance (DHI)*. The DHI also includes the portion of light reflected from the earth's surface, re-scattered by the atmosphere and incident on the surface. The amount of light reflected from the surface is dependent on the albedo. Albedo is a ratio of the irradiance intensity from the surface and incident on a surface. The albedo can range from 0 to 1 with typical values of 0.2 for ground and fresh snow can reach up to 0.8. The total amount of radiation incident on a horizontal plane is the *global horizontal irradiance (GHI)*, and is calculated as,

$$GHI = DNI * \cos(\varphi_a) + DHI \quad (7)$$

where φ_a is the solar zenith angle. Therefore, the GHI is the sum of the diffuse radiation and the cosine, between normal and solar position, component of the direct radiation from the sun. The solar radiation is a measure of power per unit area, typically watts per meter squared (W/m^2). The power is maximized when the sun is normal to the horizontal surface and falls off as the angle between the normal of the surface and the incident angle increases. In reference to Fig. 7, the components of the GHI, DNI and DHI, are shown as the atmosphere and clouds affect the light from the sun.

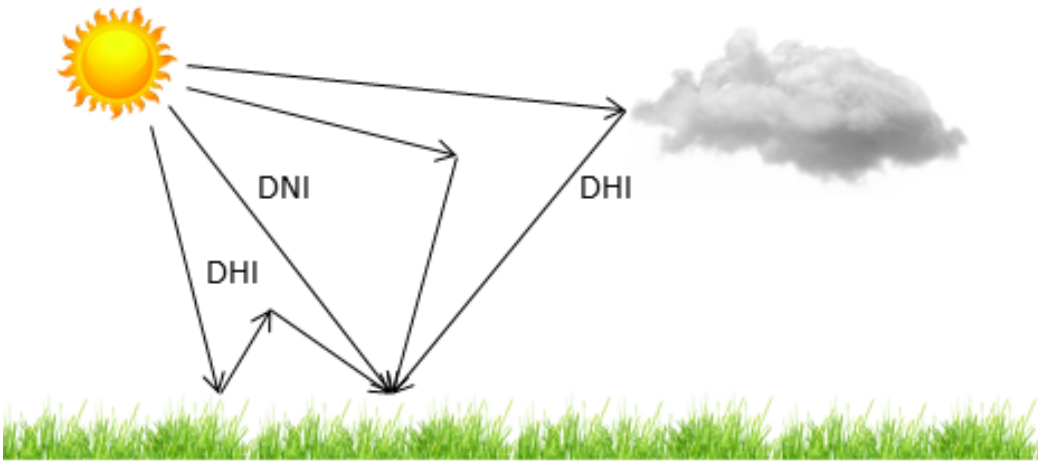

Fig. 7. The components of the total solar radiation that make up the GHI at a given point on the earth's surface. Ground reflection, scattering, and clouds increase the direct beam components from the sun.

II.VI. Terrestrial Spectral Irradiance

The terrestrial solar spectrum varies significantly with location [5]. As light propagates towards the earth's surface, atmospheric components such as clouds, ozone (0_3), water vapours (H_2O), carbon dioxide ($C0_2$), and aerosols will reduce irradiance. The extra-terrestrial irradiation spans a large wavelength range and difference components of the atmosphere affect wavelength specific regions. The amount of attenuation of these components is dependent on the density and path length, AM, of the light. The result is a highly variable filter of the extra-terrestrial spectrum depending on location and sun position. The effects of atmosphere on the extra-terrestrial spectrum can be seen in Fig. 8 where the black dotted line is attenuated by AM values of 1, 1.5, and 2.0. The AM values correspond to a sun's elevation of 90^o, 41.8^o, and 30^o, respectively. The atmospheric conditions are set to the ASTM G-173 standards set by NREL and the spectrums are generated with the Simple Model of Atmospheric Radiative Transfer of Sunshine (SMARTS).

The loss mechanism's for the AM 1.5 spectrum under ASTM G-173 condition can be seen in Table 1. Water vapour absorption is the dominant atmospheric process at 12.1% reduction of the total irradiance over the spectral range. Water vapour absorbs a wide range of wavelengths and has a strong effect in the infrared region [7]. The next significant loss mechanism is Rayleigh scattering at 10.2%. Rayleigh scattering is a dominant factor in the visible wavelength range where sunlight is scattered by the particles within the atmosphere. The aerosols, gas, and ozone further reduce by 7.1%, 1.8%, and 1.7% respectively.

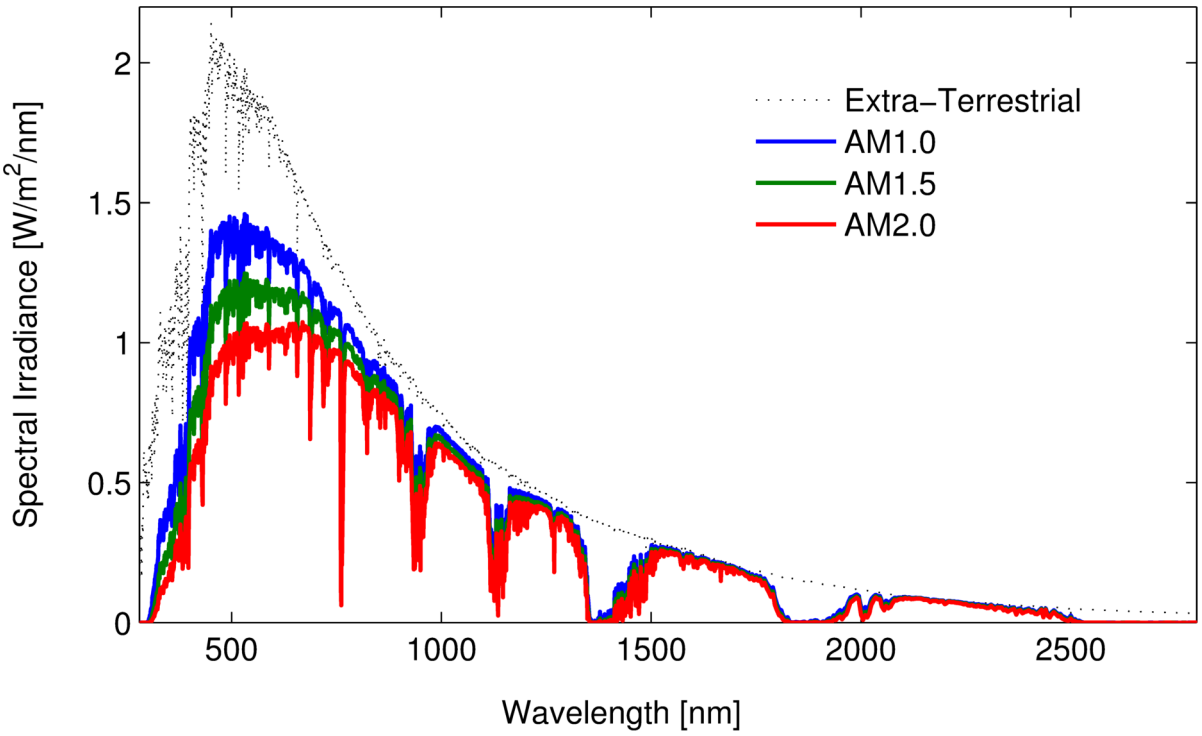

Fig. 8. The spectral irradiance of the extra-terrestrial with AM 1, 1.5, and 2.0 from 280 to 2800 nm. The unique spectral distribution for the different AM values is a result of the amount of atmosphere the sunlight will propagate through.

Table 1.Loss Mechanism of AM1.5 Spectrum due to Atmosphere absorption and scattering [9]

Loss Mechanism for AM1.5D	
Water Vapour Absorption	12.1%
Rayleigh Scattering	10.2 %
Aerosols Absorption	7.1 %
Gas Absorption	1.8 %
Ozone Absorption	1.7 %

III. Solar Radiation on a Collector

Up to now, the total amount of solar radiation has been calculated for a specific location. This next section will derive the solar irradiance on a fixed collector. For a fixed collector, the direct, diffuse, and reflected components that strike the collector can be seen in Fig. 9.The

amount of direct beam that will strike the collector is proportional to the incident angle as the sun moves through the sky. The diffuse and reflected portions are more difficult to account for since they are dependent on the surrounding environment.

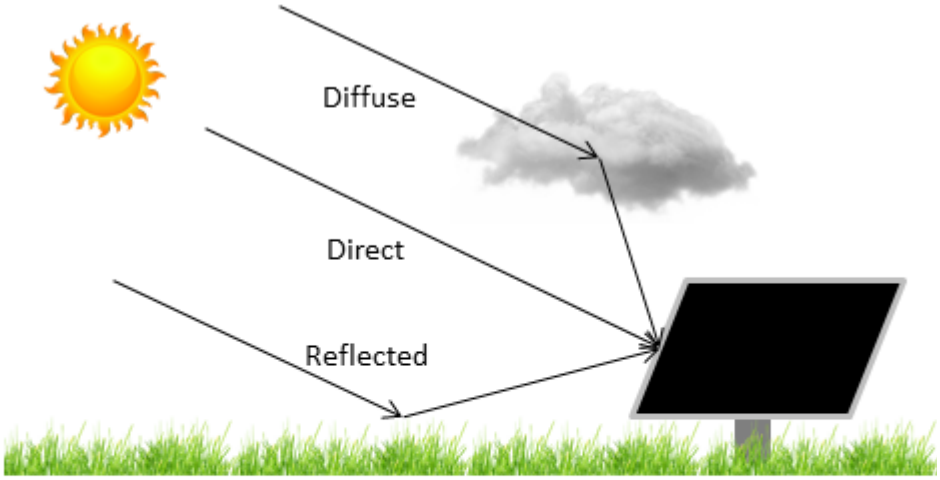

Fig. 9. Total solar radiation of a fixed collector is a combination of diffuse, direct, and reflected radiation

III.I. Direct Beam Radiation

The total radiation, I_B, is a simple conversion into the direct beam component, I_{BC}, incident on a collector through the incident angle. The incident angle, θ, is the angle between the direct beam and the normal of the collector surface [8]. The function of the direct beam component is calculated as,

$$I_{BC} = I_B cos\theta \quad (8)$$

where I_B is the total radiation, area under the spectral irradiance curve from Fig. 8, and θ is the angle of incidences. The cosine factor gives the incident portion of the beam on the collector. The incident angle is a function of the sun's position through the day. An example of the sun's position with respect to a collect can be seen in Fig. 10 where the azimuth angle, φ_s, measures the displacement from east to west and the sun's elevation angle, β, is measured from the horizon. The incident angle is calculated as [8],

$$cos\theta = cos(\beta)cos(\varphi_s - \varphi_c)sin(\Sigma) + sin(\beta)cos(\Sigma) \quad (9)$$

where φ_s is the sun's azimuth angle measured from due south, by convention is positive from angles between east and south, φ_c is the collectors azimuth angle, and Σ is the elevation angle of the collector from the horizon.

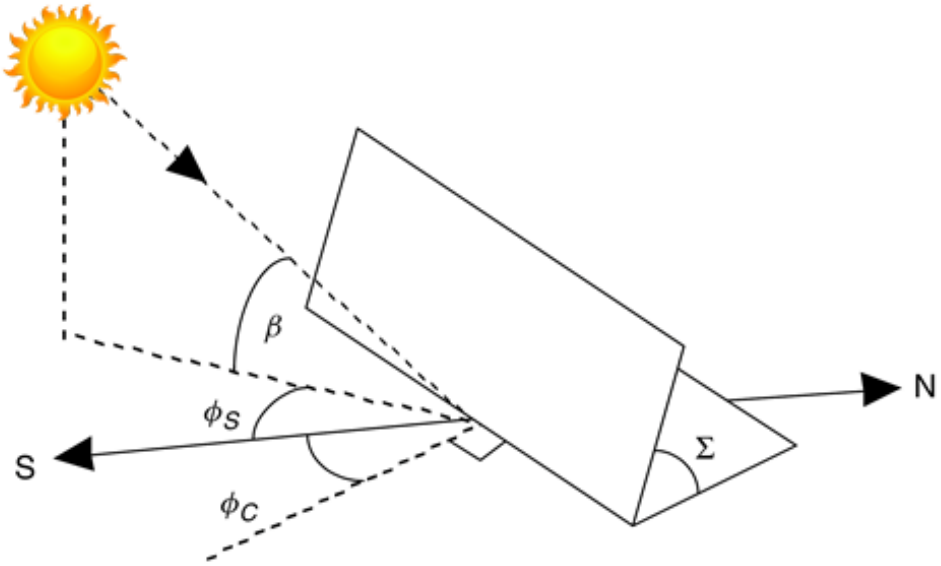

Fig. 10. An illustration of the collector, φ_c, and elevation, Σ , angles with respect to the sun position for a single time after solar noon (modified from [8])

III.II. Diffuse and Reflected Radiation

The diffuse and reflected radiations on a collector are more difficult to calculate. There are numerous components that make up the diffuse radiation. Scattering from particles and dust in the atmosphere make up the majority of diffuse beam incident on a collector. However, it is possible for diffuse light to be reflected off the ground, be re-scattered in the atmosphere then hit the collector [8]. Furthermore, on a cloudy day all the light will be diffuse. A simple model to account for the diffuse is to assume that diffuse radiation is equal from all direction about the collector, as seen in Fig. 11.a [8]. The *isotropic* model then relates the total diffuse radiation with a clarity index, C. The clarity index for a given day, n, is,

$$C = 0.095 + 0.04sin\left[\frac{360}{365}(n - 100)\right] \qquad (10)$$

Then the diffuse beam is proportional to the direct radiation with the clarity index as,

$$I_{DH} = CI_B \quad (11)$$

Equation (11) results in the total diffuse radiation on a horizontal collector, I_{DH}. With the isotropic assumption, a horizon plan "sees" the full sky. As the elevation angle of the collector angle is increases, the collector "sees" less of the sky until it reaches 50% of the sky at 90^0. This can be seen in Fig. 11.a Therefore, the diffuse radiation on an elevated collector can be calculated as,

$$I_{DC} = I_{DH}\left(\frac{1 + cos\Sigma}{2}\right) \quad (12)$$

where I_{DC} is the diffuse radiation on the collector, I_{DH} is calculated from (11), and Σ is the collects elevation.

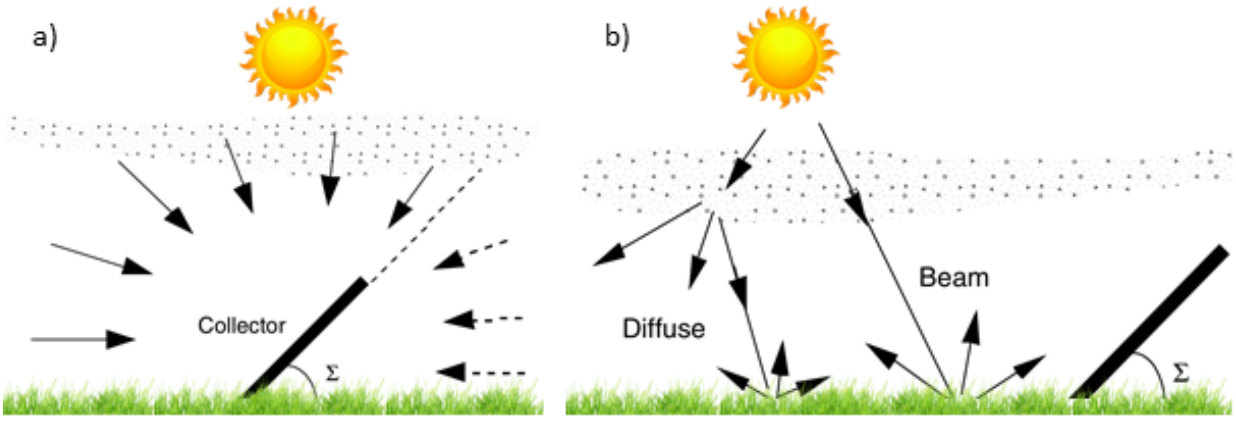

Fig. 11. The diffuse radiation proportion on the collector proportional to the total amount of sky the collector is exposed to (a). The reflected radiation from both the diffuse and direct beam reflecting off of the ground surrounding the collector (modified from[8]).

The final component of the radiation on a collector is the reflected beam. The total amount of reflected beam can considerably increase the total radiation on a collector when the surrounding environment has a high albedo. Similar to the diffuse isotropic assumption, for an area in front of the collector, of reflectivity ρ, the total amount of reflected radiation is equal magnitudes in all direction. The total amount of reflected radiation is the sum of the normal direct beam to the ground and the diffuse light [8]. For a horizontal collector, there will be no reflected beam contributing to the total insolation. As the collector angle increases, it will "see" more of the ground reflected radiation, as seen in Fig. 11.b, and reaches 50% at an elevation angle of 90^O. The total reflected beam radiation on a collector is calculated as,

$$I_{RC} = \rho(I_{BH} + I_{DH})\left(\frac{1 - cos\Sigma}{2}\right) \quad (13)$$

equivalently,

$$I_{RC} = \rho I_{BH}(sin\beta + C)\left(\frac{1 - cos\Sigma}{2}\right) \quad (14)$$

III.III. Total Collector Radiation

The total amount of terrestrial radiation is proportional to the distance between the earth and the sun, the sun's position in the sky, and the location of the observer. To demonstrate the daily variation, Fig. 12 shows the sun elevation angle and AM for June 21st in Ottawa. Ottawa has latitude of approximately 45°, resulting in a max elevation and AM value of 68.01 degrees and 1.08, respectively. In the morning and evening, low sun elevation, the AM values change rapidly due to the earths shape. When the sunbeam is close to the horizon, there is a larger path length change for small differences in elevation. As the sun get's higher in the sky, the change is path length is less intense.

With SMARTS, a terrestrial spectrum can be generated for each AM value in the day found in Fig. 12. Integrating the spectrum along with tracking the total amount of sun radiation incident on a fixed tilt collector with equations 8, 12, and 14 for the direct, diffuse, and reflected radiation components is now a simpler calculation. In reference to Fig. 13, the radiations for all three components were calculated for June 21st for a collector set to 45° elevation and 0° azimuth. From sunrise, 04:21, till 06:05 the direct beam from the sun is behind the collector since the sunrise is in the Northeast. Therefore, the diffuse light governs the Ic curve. A similar trend can be seen after 17:45 when the sun is in the Northwest. However, once the sun is in front of the collector. The total radiation on the collector from Fig. 13, area under I_c, is 464.37 kW/m^2. The direct, diffuse, and reflected contribute 80.35%, 16.22%, and 3.42%, respectively of the total radiation.

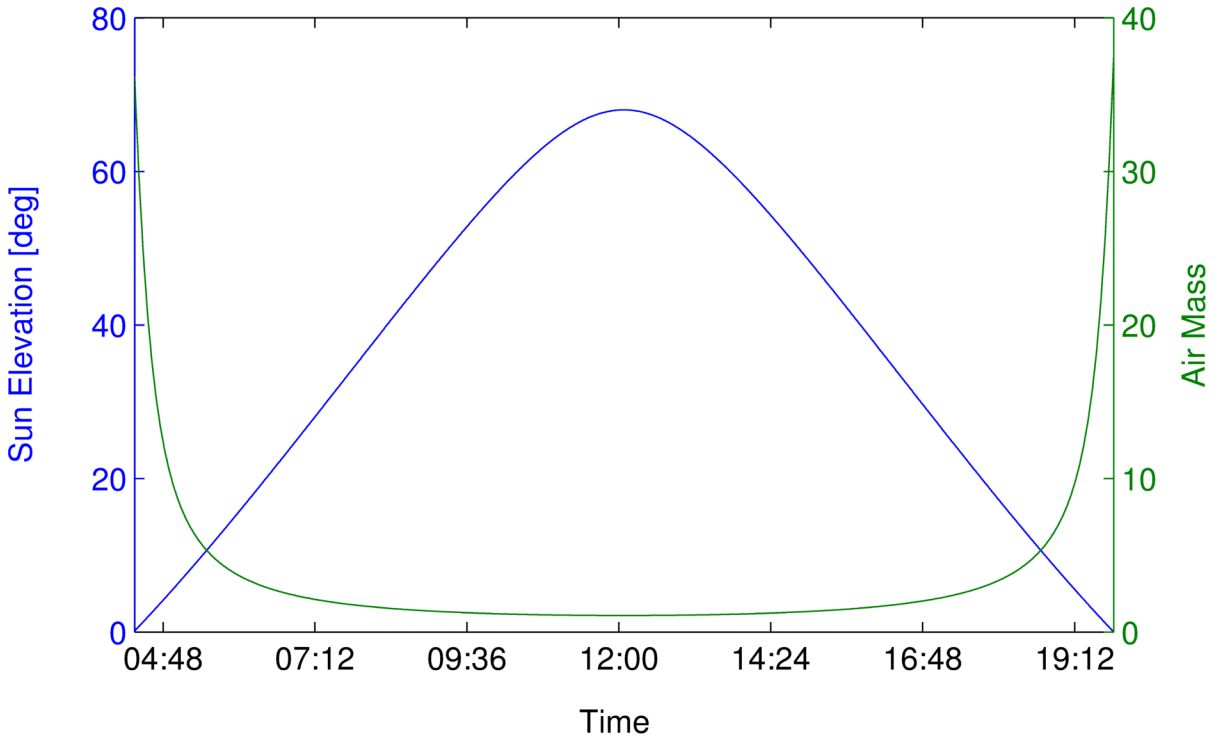

Fig. 12 The sun's elevation angle, blue, and the AM, green, values for June 21st in Ottawa, latitude 45o.

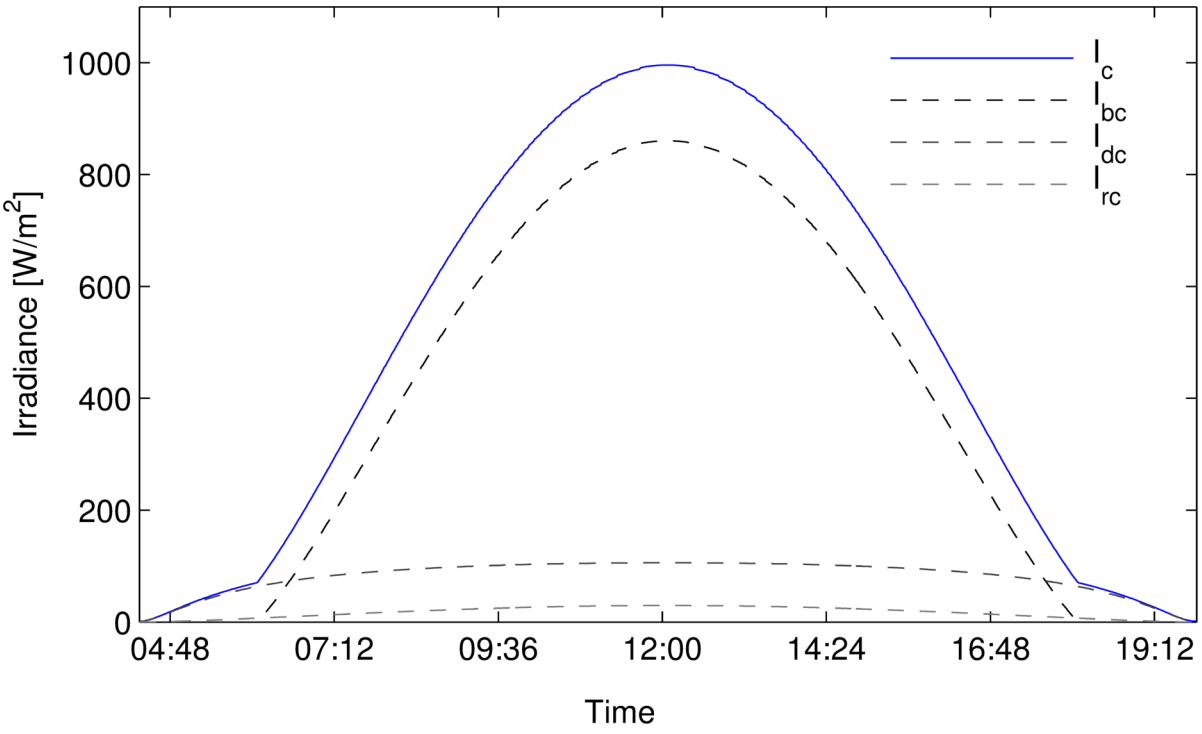

Fig. 13. The direct (I_{bc}), diffuse, and reflected components of the total radiation for a 45o elevated fixed collector with a azimuth of 0o located in Ottawa on June 21st. Total radiation of 464.37 kW/m2.

In Fig. 13, the collector was set to an arbitrary angle of 45°, for first order approximate, setting the collector to the latitude will optimize the output since the collector will be perpendicular to the sun's rays at solar noon on the equinoxes [8]. Refer to section Optimal Collector Angle for a Single Day for the optimal elevation angle of the collector so a single day. In reference to Fig. 14, the total radiation for a collector can be seen when the elevation angle is set from 0° to 90°. The total output of a panel can vary significantly with the different elevation angles. When the panel is horizontal, it collects all the diffuse light without the reflected beam. As the panel elevates, more of the reflected beam is captures at the expense of less diffuse light. In comparing the output of a horizontal, black, and vertical, mauve, collector in Fig. 14 the total radiation is 533.19 kW/m^2 and 213.02 kW/m^2, respectively. Therefore, angles that collect more diffuse light is more favourable.

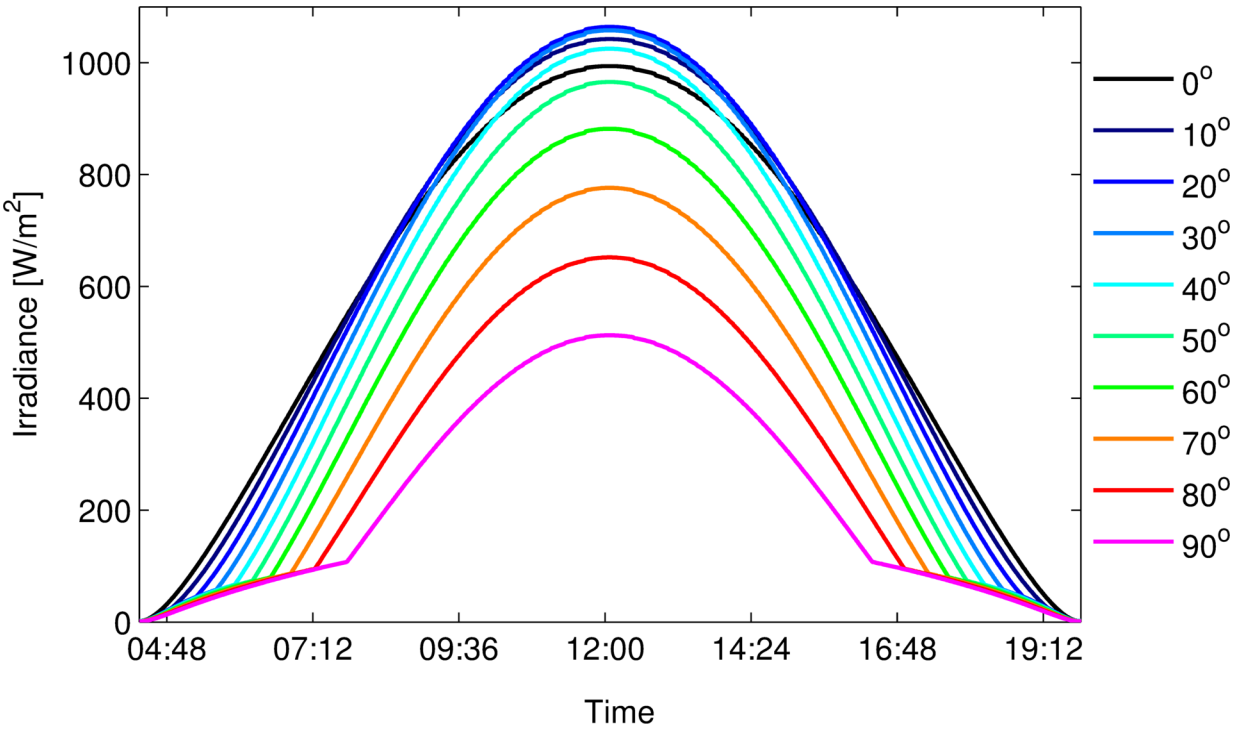

Fig. 14. Total radiation, I_c, for increasing elevation angles of a collector on June 21st. The horizontal collector has a higher peak than vertical due to

IV. Optimization of Fixed Tilt PV System

Now the resource for a fixed collector at all possible elevation angles has been assessed, the output of a flat panel PV system can be optimized to generate the highest return of investment. This section will describe a typical 10 kWh system deployment in Ottawa and calculate the optimal amount of times and durations to maximize the output of the system.

IV.I. Photo Voltaic Systems

A grid connected PV system can either be ground or roof mount for small-scale personal investments. However, the latter is more restricted since a house may not face the ideal direction and the roof limits the range of possible elevation angles. Refer to section Optimization for Collector Azimuth Angle for losses if the collector is not facing south. This section will analyse the output of a ground mount PV system with adjustable elevations from 0^o to 90^o.

The main types of silicon used in PV modules are mono-crystalline, and multi-crystalline silicon. A mono-crystalline, mono-Si, is a semiconductor material with a continuous crystal structure through out the materials. The drawback is a slow and careful manufacturing process giving rise to higher cost [12]. Multi-crystalline silicon does not have a continuous crystal structure, the intersections of the different structures creates gain boundaries. These boundaries give rise to dark and light regions on the cell. The two bare cells can be seen in Fig. 15. The gain boundaries create localized recombination regions and reduce the carrier lifetime within the material [10]. Recent development in production has greatly reduced the cost for multi-crystalline solar panels. Furthermore, the manufacturing process for multi-crystalline results in a square cells. Therefore, a multi-crystalline module will have a higher Si area, seen in Fig. 16.

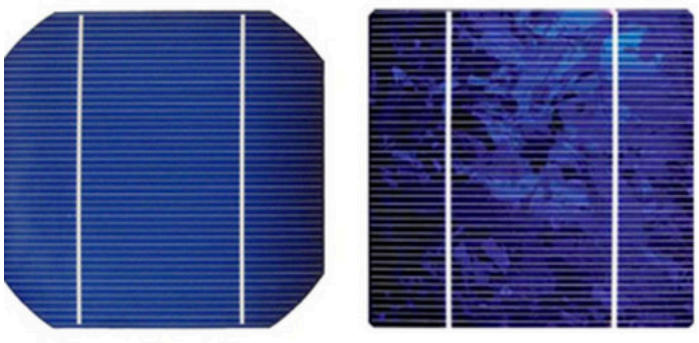

Fig. 15. Mono- and Multi-crystalline silicon bare cells on the left and right, respectively.

The module for the system is a 72 multi-crystalline silicon cell connected in series. Resulting in maximum voltage and current of 44.9V and 8.3A. Under standard test conditions, total irradiance of 1000 W/m^2, cell temperature at 25^0, and AM1.5G spectrum, the module efficiency is 15.6%. This full module description can be seen in Fig. 16.

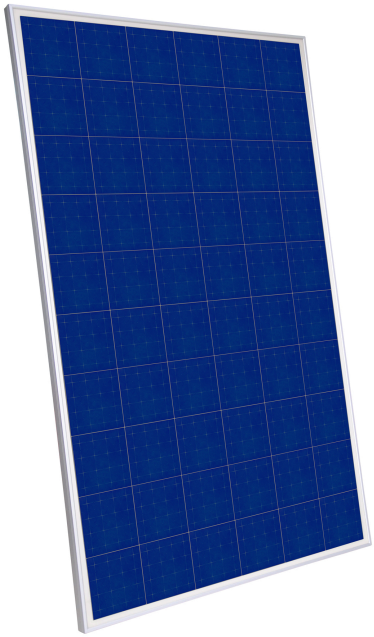

Characteristic	
Efficiency [%]	15.6
Short Circuit Current [A]	8.9
Open Circuit Voltage [V]	44.9
Maximum Power Point Voltage [V]	34.4
Maximum Power Point Current [A]	8.2
Number of Cells per Series sting	6x12
Module dimension [mm]	1970x990x50
Nominal power [W]	280
Number of Modules	38

Fig. 16. Multi-crystalline silicon module with 6x12 series connected cell (LEFT). Module characteristics (RIGHT) [13]

IV.II. Feed In Tariff Model

In Ontario, the micro Feed In Tariff (microFIT) program began in 2009 to increase renewable energy generation [13]. MicroFIT encourage residential deployment of renewable energies project that are less than 10kW. Under a microFIT contract, the owner is guaranteed a price per kWh for 20 years and projects can be either solar, wind, water, biomass, biogas, or landfill gas. The price schedules for the projects that fall under the microFIT scope are in Table 2. The prices are set in order to gain back, through revenues, the capital cost and a reasonable return on investment. In the previous section, the nominal power for the panels was 280 Watts with 36 panels resulting in an output of 10,640 Watts. The extra power will account for inverter, max power point tracker, and variations in insolation in order to maximize the output. In reference to Table 2, the price for the non-rooftop solar (PV) under 10 kW is 0.289 $/kWh.

Table 2. microFIT / FIT Price Schedule [14]

Renewable Fuel	Project Size Tranche*	Price (¢/kWh)	Escalation Percentage**
Solar (PV) (Rooftop)	≤ 10 kW	38.4	0%
	> 10 kW ≤ 100 kW	34.3	0%
	> 100 kW ≤ 500 kW	31.6	0%
Solar (PV) (Non-Rooftop)	≤ 10 kW	28.9	0%
	> 10 kW ≤ 500 kW	27.5	0%
On-Shore Wind	≤ 500 kW	12.8	20%
Waterpower	≤ 500 kW	24.6	20%
Renewable Biomass	≤ 500 kW	17.5	50%
On-Farm Biogas	≤ 100 kW	26.3	50%
	> 100 kW ≤ 250 kW	20.4	50%
Biogas	≤ 500 kW	16.8	50%
Landfill Gas	≤ 500 kW	17.1	50%

IV.III. Optimal Collector Angle for a Single Day

The optimizing the collector elevation angle will result in a panel to harness the highest potential of energy from the sun. A driving factor in the optimization process is the variations in the sun's position and the elevation angle has a large degree of daily and seasonal fluctuation. For example, the sun reaches a maximum elevation of 68.02^0 and 21.14^0 for June 21st, and December 21st. In order to select the optimal angle, the total insolation as a function of elevation angle must be calculated. The total insolation for a specific angle is the integral of an individual curve from Fig. 14. The total insolation for a collector positioned at 0^0 to 90^0 on both June 21st and December 21st can be seen in Fig. 17. In reference to Fig. 17, the red points signify the optimal angle and are 10^0 and 70^0 for the summer and winter solstice, respectively. The reason for the higher elevation angle in the winter is do to low sun elevation angle. Furthermore, the seasonal variation has a significant impact on the total amount of potential energy. For the winter, under optimal conditions, the maximum total insolation of a collector is 225.68 kW/m^2. In comparison, to June 21st has a maximum insolation of 539.52 kW/m^2 at 10^0 elevations. If the collector elevation angle is set to 10^0, on December 21st the insolation on the collector would be 113.53 kW/m^2. Resulting in a loss of 50.3% from the optimal position. Similarly, if the angle were to be set to at 70^0, on June 21st the potential insolation will drop to 338.52 kW/m^2, amounting to a loss of 62.7%. Therefore, the optimization must take into account more than a single day.

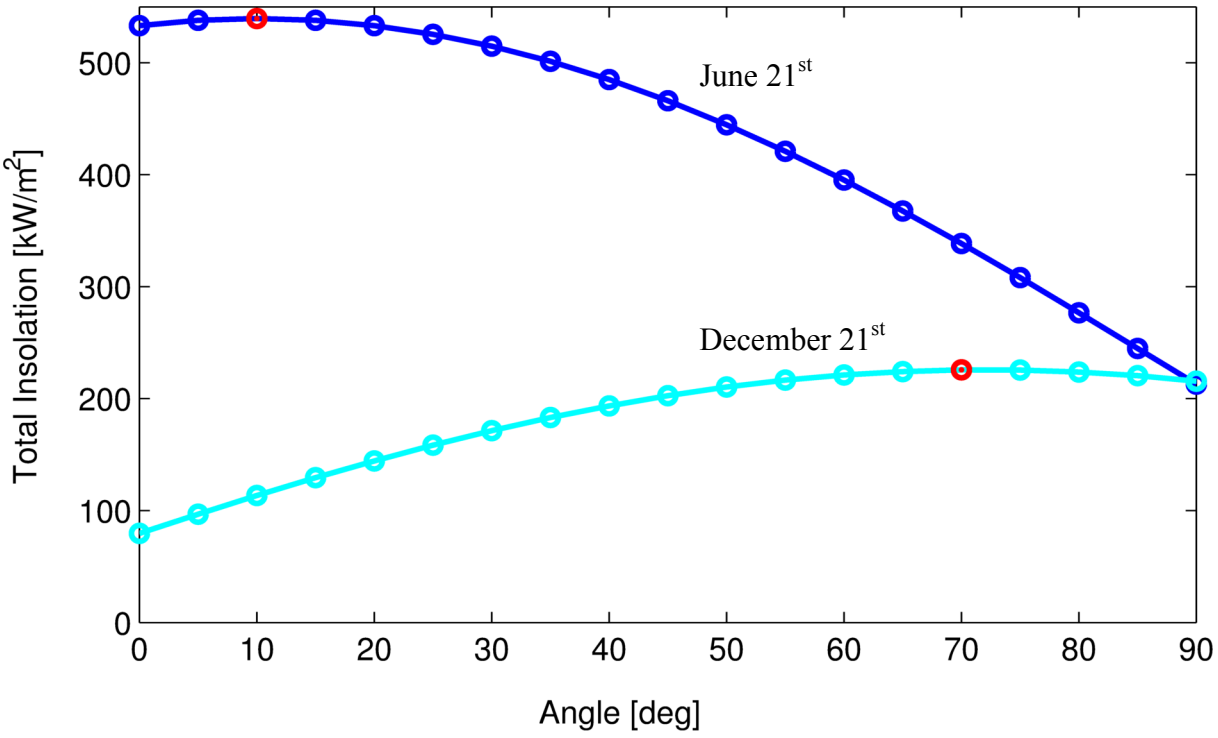

Fig. 17. Total insolation on a collector on June 21st, blue, and December 21st, cyan, as a function of elevation angle. The optimal angle, red, is 539.52 kW/m^2 and 225.68 kW/m^2 at 10^0 and 70^0, respectively.

IV.IV. Optimal Set Dates and Angles for a Full Year

Calculations for the optimal collector angle of a single day were performed in the previous section. However, there are considerable losses unless a larger time span is taken into consideration. The simplest step is to optimize for a single angle that will result in the highest amount of insolation for a full year, 365 days. The annual insolation for the system is shown in Fig. 18 for the range of collector angles. In reference to Fig. 18, the optimal elevation angle is 39^0 and the result is a total of 133.61 MW/m^2 of sun on a collector under this condition. For the system, the annual revenue is then $11,474.50. Under any other angle, there will be lower revenue for the system. Changing the collector's elevation angle multiple times in the year can further increase the total revenue. Fig. 19 shows the annual revenue for the amount of optimal angles used in a year. In reference to Fig. 19, the annual revenue for two optimal angles set in a year is $12,025.90. Therefore, resulting in a gain of $551.40 and 4.81% in annual revenue and potential insolation on the collector, respectively. Furthermore, a gain in annual revenue of $709.70 or 6.19% is the plateaus at 52 angles. Refer to Appendix A: Table of Optimized Dates for Variable Fixed Angle Panel for the detailed results of Fig. 19.

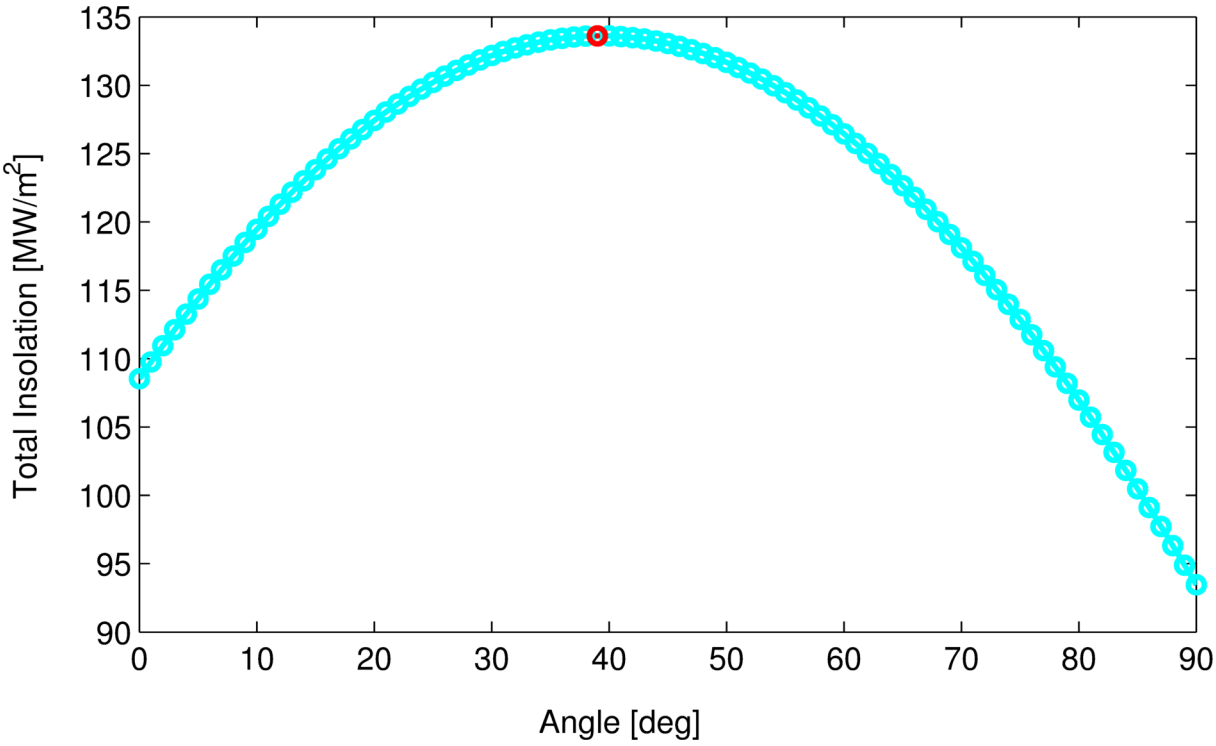

Fig. 18. The total insolation on a collector as a function of its elevation angle for a full year deployment. The Optimal angle, red, is 39^0 at 133.61 MW/m^2.

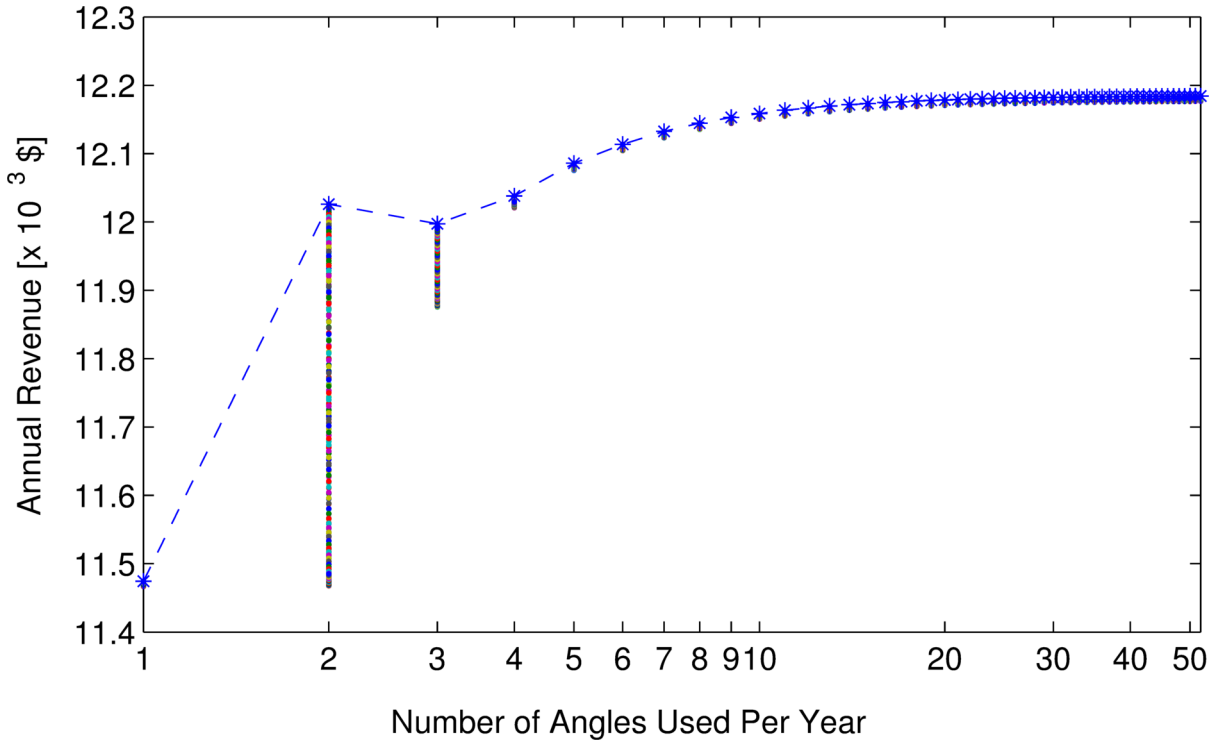

Fig. 19. The annual revenue for a 10kW system for the amount of optimal set angles used within a year. The small dots represent the annual revenue for different start dates in the year. An annual revenue gain equivalent to $551.40 is for one to two angles and a max of and $709.70 for 52 angles.

IV.V. Optimization for Collector Azimuth Angle

Depending on the environment surrounding the system, they maybe object that will shadow the panels for a portion of the day. Shading limits the potential amount of sunshine a panel can harness into electricity [11]. With a ground-mounted system, there is freedom to install the collectors facing a different direction. This can help alleviate the losses of shading objects. However, there is a loss in the amount of potential energy, calculations from section *III.III* Total Collector Radiation with $\varphi_c \neq 0$. The loss in annual revenue can be seen in Fig. 20for collector azimuth angles +/-5^0, 10^0, 15^0, and 20^0. In reference to Fig. 20, the absolute loss in annual revenue is \$15.00, \$59.70, \$133.60, and \$234.90 for an azimuth angle of +/-5^0, 10^0, 15^0, and 20^0, respectively. However, exploiting the multiple elevations angles can reduce the loss in revenue. For example, the annual revenue for two optical set angles is equivalent to that of six for a collector azimuth angle set to +/- 10^0. Therefore, setting the collector angle six times a year will have the same revenue of an ideal collector set only twice a year.

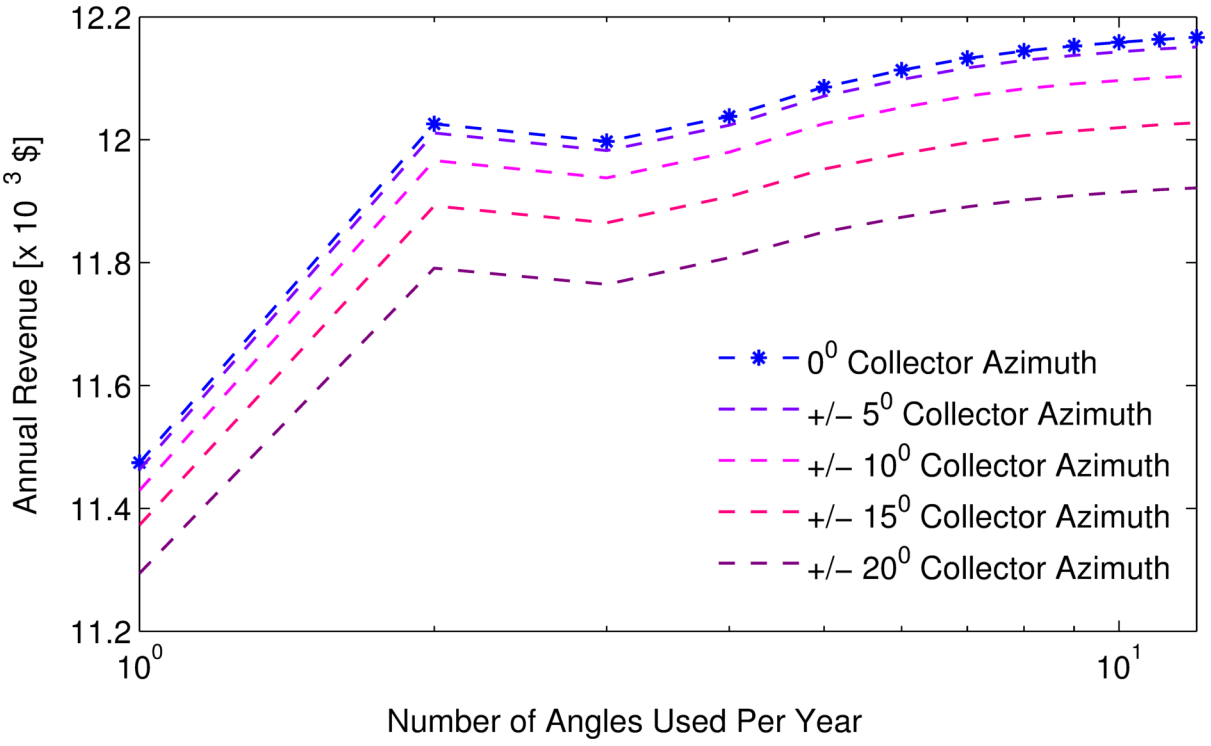

Fig. 20. The annual revenues for a 10kW system with collector azimuth angles set to +/-5^0, 10^0, 15^0, and 20^0 as a function of the total amount of optimal set angles used within a year. An absolute loss in annual revenue of \$15.00, \$59.70, \$133.60, and \$234.90, respectively

V. Conclusion

A 10kW ground mounted variable tilt PV system can be optimized to provide considerable gains and mitigate losses in annual revenue. In optimizing the set dates and corresponding collector elevation angle the amount of penitential energy can be maximised. A system that operates with two optimal angles will have an increase of 4.81% over a single set angle. Furthermore, a system has the potential to increase the total amount of energy by 6.19% with a larger set of angles set within a year. The gain in annual revenue for these two options is $551.40 and $709.70, respectively. Finally, the loss in annual revenue for location where the collector cannot face the optimal angle, which can amount up to $234.40, can now be earned. In exploiting more optimal set angles, the system will collect more energy thereby eliminating the loss. Although the increase in revenues is specific to this system, the percentages for the increase energy can be applied to other systems.

References

[1] J. Nyboer, N. Melton, and S. Goldberg, "Renewable Energy in Canada," Canadian Industrial Energy End-use Data and Analysis Center, Simon Fraser University, Burnaby, BC, March 2014

[2] L. Freris, D. Infield, "Renewable energy in power systems," John Wiley & Sons, Ltd; 36-37, 2008

[3] T. Stoffel, D. Renné, D. Myers, S. Wilcox, M. Sengupta, R. George, C. Turchi, "Concentrating Solar Power: Best Practices Handbook for the Collection and Use of Solar Resource Data," Technical Rerport, NREL/TP-550-47465, September 2010

[4] Christien A. Gueymard, "The sun's total and spectral irradiance for solar energy applications and solar radiation models," Solar Energy 76, 423-452, 2004

[5] F. Vignola, J. Michalsky, T. Stoffel, "Solar and Infrared Radiation Measurements", CRC Press, Taylor & Francis Groups, 2012

[6] I. Reda, A. Andreas, "Solar position algorithm for radiation applications," Solar Energy, vol. 76, pp. 577-589, 2004

[7] C. Gueymard, "Parameterized Transmittance Model for Direct Beam and Circumsolat Spectral Irradiance," Solar Energy, vol. 71, no.5, pp. 325-346, 2001

[8] G. M. Masters, "Reneable and Efficient Electric Power Systems," Wiley-Interscience, John Wiley & Sons, 2014

[9] V. Tatsiankou, "Instrumentation Development for Site-Specific Prediction of Spectral Effects on Concentrated Photovoltaic System Performance," University of Ottawa, 2014

[10] C. Honsber, S. Bowden, "PVCDROM," ASU Solar Power Lab, 2015

[11] T. M. Klucher, "Evaluation of models to predict insolation on a tilted surfaces," Solar Energy, vol. 23, pp. 111-114, 1979

[12] "Handbook of Photovoltaics Science and Engineering," John Wiley and Sons, 2011

[13] "microFIT Program," Independent Electricity System Operator, http://microfit.powerauthority.on.ca/, 2015

[14] microFIT, "FIT/microFIT Price Schedual (Effective September 30th, 2014 and January 1st, 2015 for microFIT," Independent Electricity System Operator, 2014

Appendix A: Table of Optimized Dates for Variable Fixed Angle Panel

Optimal Angles Used	Set Date	Collector Elevation [deg]
1	N/A	39
2	September 24th	62
	March 25th	23
3	December 22nd	55
	April 22nd	17
	August 22nd	54
4	November 11th	70
	Febuary11th	42
	May 13th	14
	August 12th	46
5	December 19th	67
	March 2nd	37
	May 14th	13
	July 26th	34
	October 7th	65
6	November 9th	70
	January 8th	64
	March 10th	37
	May 10th	13
	July 10th	23
	September 9th	53
7	November 17th	71
	January 8th	66
	March 1st	44
	April22nd	19
	June 13th	13
	August 4th	33
	September 25th	58
8	November 30th	72
	January 14th	65
	March 1st	46
	April 15th	22
	May 31st	11
	July 16th	22
	August 30th	45
	October 15th	64
9	December 10th	72
	January 19th	65
	March 1st	47
	Spril 10th	26
	May 21st	12
	June 30th	15
	August 10th	33

	September 19th	54
	October 30th	68
10	November 12th	70
	December 18th	71
	Janury 24th	64
	Match 1st	48
	April 7th	29
	May 13th	14
	June 19th	12
	July 25th	24
	August 31st	43
	October 6th	60
11	November 22nd	71
	December 25th	71
	January 27th	64
	March 1st	49
	April 3rd	32
	May 6th	16
	June 9th	11
	July 12th	18
	August 14th	33
	September 16th	51
	October 19th	64
12	December 1st	72
	December 31st	70
	January 30th	63
	March 2nd	49
	April 1st	33
	May 2nd	18
	June 1st	11
	July 1st	14
	August 1st	26
	August 31st	42
	October 1st	57
	October 31st	67